An Experimental Comparison of Transmission Vibration Responses from OH-58 and AH-1 Helicopters

Edward M. Huff
NASA Ames Research Center
Moffett Field, CA 94035
ehuff@mail.arc.nasa.gov

Irem Y. Tumer
NASA Ames Research Center
Moffett Field, CA 94035

Marianne Mosher
NASA Ames Research Center
Moffett Field, CA 94035

ABSTRACT

Statistical analyses of transmission vibration patterns from an AH-1 Cobra helicopter were previously reported. Fourteen steady-state maneuvers were analyzed using multi-factor analysis of covariance. Based on triaxial recordings, it was found that only two maneuvers displayed reliably stationary time-series: low and high power forward climb. Principal Components Analysis of the triaxial RMS data was shown to aggregate a large portion of variance associated with engine torque on the fist component. In the present study the experimental procedures were repeated on an OH-58c Kiowa helicopter. Statistical results are compared with those from the earlier study, and also with data from the Glenn Research Center OH-58c transmission test facility. Analyses are also included of the comparative frequency responses of these three transmission systems, and general conclusions are drawn with regard to HUMS design requirements. Finally, future research directions are summarized for in-flight HUMS research using NASA/Army aircraft and transmission test facilities.

INTRODUCTION

At the AHS 2000 Forum, Huff, Barszcz et al. [1] reported an experimental analysis of vibration responses recorded from a surrogate Apache, AH-1 Cobra helicopter. In that study, 14 steady-state flight maneuvers were flown by two pilots and compared with regard to signal RMS. Using triaxial accelerometer recordings, it was shown that only two maneuvers resulted in a high percentage of stationary recording epochs: forward climb flown at low and high power. Contrary to expectation [2-4], low and high-speed forward flight proved to be disappointing with regard to signal stationarity.

In the Cobra study, the RMS values per shaft revolution of triaxial vibration data recorded at the planetary ring (annulus) gear were de-correlated using Principal Components Analysis (PCA). Scores on each of the orthogonal components were then analyzed separately using multivariate linear regression techniques. Based on a fixed-effects analysis of covariance (ANCOVA), it was shown that the leading principal component, PC-1, aggregated a very large percentage of variance induced by engine torque, and that PC-2 and PC-3 primarily contained variance due to experimental main effects and interactions, respectively. Thus, there was suggestive evidence that the transmission's surface vibration pattern contains directional information that may prove useful in future damage detection algorithms.

At the AHS-2000 Forum Huff, Tumer, et al. [5] also reported the first of a two-phase study that examined the effects of torque, mast-lifting, and mast-bending forces on the vibration responses of an OH-58c transmission in the NASA Glenn Research Center (GRC) 500 HP Transmission Test Facility. Vibration signals were obtained from various locations, and 34-sec. recordings were made specifically at the annulus to correspond with data to be collected at a later date on the Ames aircraft. In addition, one channel of data was recorded using an accelerometer bracket that was the design prototype for both uniaxial and triaxial accelerometer brackets used on the Ames aircraft. Thus, data were available from the earlier study to allow comparisons between test rig and aircraft.

Presented at the American Helicopter Society 57th Annual Forum, Washington D.C., May 9-11, 2001. **Copyright © by the American Helicopter Society. All rights reserved.**

OBJECTIVES

Like the AH-1 Cobra study reported previously, the present OH-58 Kiowa flight experiment is designed to reveal the extent to which steady-state maneuvers influence characteristic vibration patterns measured at planetary gear locations of the main transmission. In order to generalize the previous findings, the experimental conditions and procedures were replicated as closely as possible on the OH-58 research helicopter.[1]

Given that data would now be available from two aircraft, a major objective was to compare OH-58c triaxial vibrations with those from the AH-1 study. Although the AH-1 updates several attitude parameters on a 1553 bus, it was only possible to record engine torque on the OH-58. Fortunately, since torque is known to be the dominant correlate of vibration signal energy, this minimal instrumentation is considered adequate for inter-aircraft comparison purposes. A measure of rotor RPM was also obtained from the data count between tachometer pulse markers.

A second major set of objectives was to compare uniaxial aircraft data with prior baseline results from the OH-58 test rig [5], and with radial (i.e., z-axis) recordings from the triaxial accelerometer used in the present study. In addition to global RMS comparisons, there is particular interest in the frequency content of the signals, and how it relates to internal mesh frequencies and their higher harmonics.

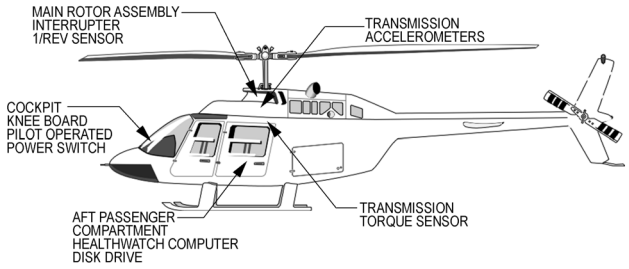

Figure 1. Ames OH-58 *HealthWatch* System Installation

[1] Both aircraft are located at NASA -Ames Research Center (ARC) and operated by the US Army.

METHOD

Instrumentation

The OH-58c was instrumented as shown in Fig. 1. The M/S DOS based HealthWatch data acquisition system, previously used on the AH-1 Cobra, was adapted for this application by shock mounting it in the aft passenger compartment using a special flight-approved pallet. As was done with the Cobra, this apparatus is used to record eight-channels of analog signals: six channels are dedicated to vibration recording; one channel is used to sample engine torque; and one channel is used to sample a once-per-revolution tachometer pulse from the rotor shaft.[2] Three of the vibration channels (A4, A5, and A6) are connected to an Endevco 7253A-10 triaxial accelerometer with a natural frequency of 80kHz. Unlike the AH-1, which used two such units, on the OH-58 three channels (A1, A2, and A3) are connected to Endevco Model 7529A-10 single-axis accelerometers. Gains on the signal conditioning board were set to 72g for channels A1, A2, A3, and A6, and 140g for channels A4 and A5. At these settings, clipping did not occur.

Figure 2. Accelerometer Mounting Bracket

Using specially machined, cadmium-plated mounting brackets (Fig. 2), all accelerometers are attached to existing vertical studs surrounding the transmission housing. Fortunately, there was enough exposed threading to allow the retaining nuts to be removed and re-torqued over the bracket flanges. A special installation jig was also fabricated and used to align the brackets perpendicular to the tangent line within ±2 degrees.[3] In this configuration, the three uniaxial accelerometers are radially oriented to the annulus. The triaxial accelerometer is positioned with the x-axis parallel to the rotor shaft, y-axis tangent to the annulus gear, and the z-axis radial to the annulus gear. Taking into consideration the 22kHz estimated resonant frequency of the mounting bracket, an appropriate order anti-aliasing filter (18kHz) was used in combination

[2] The standard AVA maintenance kit is used for the tachometer.
[3] Duplicates of the finished brackets and the alignment jig were provided to GRC for future research.

with a fixed per-channel sampling rate of 50kHz on all channels to satisfy the Nyquist sampling conditions.[4]

Experiment Design

In the earlier Cobra experiment, during Set 1 (i.e., the first four flights) one of the triaxial accelerometers was mounted near the input pinion and moved to a new location at greater distance from the input pinion (and engine) during Set 2 (i.e., the second four flights). In addition, Sets 1 and 2 were separated in time by approximately six months. In the present study the accelerometers were not moved, and Sets 1 and 2 (i.e., all eight flights) were conducted in the same timeframe. Although no important differences between the Sets were found in the first study, the distinction is retained and may be thought of as a pilot habituation variable. In all flights the same two test pilots flew the aircraft in 14 different steady-state maneuvers (Table 1), according to a pre-determined Latin Square matrix schedule designed to counterbalance random wind conditions, ambient temperature, and fuel depletion (Table 2).[5] Maneuvers were scheduled to last 34 seconds, in order to allow sufficient revolutions of the planetary gears to occur to apply candidate signal decomposition techniques.[6] During the experiment, therefore, 168 raw data records were obtained of 34-sec. each: — 14 flight maneuvers, flown by two pilots, on six separate occasions.

Table 1: Aircraft Maneuvers

Maneuver	Name
A	Forward Flight, Low Speed
B	Forward Flight, High Speed
C	Sideward Flight Left
D	Sideward Flight Right
E	Forward Climb, Low Power
F	Forward Descent, Low Power
	Flat Pitch on Ground
H	Hover
I	Hover Turn Left
J	Hover Turn Right
K	Coordinated Turn Left
L	Coordinated Turn Right
M	Forward Climb, High Power
N	Forward Descent, High Power

[4] No changes were made in the filter design or sampling rates from the Cobra study.
[5] The same two pilots (LH and MD) flew the Cobra experiment.
[6] Due to higher rotor speed, 32 revolutions are used per replication for the OH-58, as opposed to 28 used earlier for the AH-1.

Data Reduction

As was done in the Cobra experiment, the data were reduced in two stages. Each stage produced highly compressed summary statistics, which are archived and available for continued analyses. In the first stage, the basic statistical time domain properties of each 34-sec. recording of raw flight data were consolidated into summary matrices (SMs) on a revolution-by-revolution basis. Since each shaft revolution took approximately 0.2 sec., and sampling occurred at 50 kHz, approximately 10,000 data points were compressed into each summary statistic in these matrices. To perform analyses on an experiment-wide basis, the second stage of data reduction involved consolidating selected parameters into an experiment data matrix (EDM). The rows (i.e., statistical "cases") in the EDM are organized as treatment replications in the experiment design.

Because it does not compare logically with in-flight maneuvers, condition G (Flat Pitch on Ground), was set aside for other uses. Although four hover recordings were made during each group of two flights for each pilot, it was further decided to suppress the last hover. All flight conditions, therefore, were uniformly represented in the EDM by three ordered observations. To examine time-series variability within the recording periods shown in Table 2, summary statistics were computed separately for successive groups of 32 revolutions. These are treated as six ordered "replications" within each condition. For each such replication, the average number of runs above and below the RMS median for the 32 revolutions was also retained for within-replicate stationarity analysis. Finally, as in the earlier Cobra study, Principal Component Analysis (PCA) scores were retained that were computed from the Log(RMS) values of the triaxial channels. A single PCA was done for the experiment as a whole, rather than on a treatment-by-treatment basis.

Underlying Statistical Concepts

Based on *Parseval's theorem* [6], the Mean Square (MS) of a time domain signal is equal to its total power in the frequency domain. Since total power represents the sum of the energy over all frequencies in the spectrum, observed differences in MS (or its root, RMS), probably reflect differences in the *relative* strength of the frequency components. The only instance when this would not be true is the circumstance where the power at all frequencies changes by a proportional amount. For this reason, RMS was selected as an appropriate variable to study the global effects of flight conditions.

Table 2: Protocol for Maneuvers in Each of Two Flight Sets

		Obs. Order	Ground & Hover		Primary Flight Maneuvers						Hover & Ground	
Pilot 1	Flight 1	1	G	H	A	B	C	D	E	F		
		2			B	C	D	E	F	A		
		3			C	D	E	F	A	B	H	G
	Flight 2	1	G	H	I	J	K	L	M	N		
		2			J	K	L	M	N	I		
		3			K	L	M	N	I	J	H	G
Pilot 2	Flight 3	1	G	H	D	E	F	A	B	C		
		2			E	F	A	B	C	D		
		3			F	A	B	C	D	E	H	G
	Flight 4	1	G	H	L	M	N	I	J	K		
		2			M	N	I	J	K	L		
		3			N	I	J	K	L	M	H	G

Signals having the same RMS value, however, do not necessarily have the same underlying power spectrum, and conditions that change RMS by an equivalent amount may produce different spectra. These effects require detailed analyses of the spectral components, which can be related to RMS analysis using the fundamental relationships:

$$MS = (RMS)^2 = \mu^2 + \sigma^2 = \sum_{i=0}^{N/2} P_i$$

$$\mu^2 = P_0 = 0$$

where μ and σ are the mean and standard deviation of the infinite time series, respectively, P_i is the power of the i^{th} frequency band in the periodogram, and $N/2$ is the number of bands. For a vibration signal the mean is zero. Therefore, by substitution and induction:

$$MS = (RMS)^2 = \sigma^2 = \sum_{i=1}^{N/2} P_i = \sum_{i=1}^{N/2} \sigma_i^2$$

and, for $0 < i \le N/2$

$$P_i = \sigma_i^2$$

From this perspective, frequency analysis is a decomposition of the signal variance, σ^2, which is separated into components associated with individual frequencies. A corollary is that the variance and degrees-of-freedom, df, associated with any *set* of vibration source frequencies can be expressed as:

$$\sigma^2_{Source} = \sum_{i \ni Source} P_i = \sum_{i \ni Source} \sigma_i^2$$

$$df_{Source} = 2 \sum_{i \ni Source} df_i$$

In other words, component variances may be grouped by mesh frequencies, harmonics, sidebands, etc., by adding together power from the appropriate frequency bands. Each frequency band is associated with two degrees-of-freedom due to the symmetry of the discrete Fourier transform.[7]

As described above, the triaxial accelerometer data were first converted to PCA scores [7]. This process analytically rotates the axes to account successively for the largest percentage of remaining variance. In order to apply subsequent Analysis of Covariance (ANCOVA), however, it is necessary to apply the PCA to Log(RMS) [8, 9]. Being a non-linear transformation this is clearly not the same as applying the analyses to the original RMS values and should, therefore, only be regarded as an analytical device. Other work reported recently by Tumer and Huff [10] use PCA of synchronously averaged data in the time domain to uncover signal analysis advantages of optimized linear combinations of triaxial recordings.

Fixed-effects ANCOVA models are reported below to determine the relative importance of treatment combinations, and the extent to which engine torque and rotor speed (RPM) account for variability in the RMS scores. A fixed-effects model is used because it

[7] The last band, $P_{N/2}$, has only one degree of freedom.

allows parsing the total sum-of-squares around the global mean of the experiment on an additive basis [8]:

Total SS = Covariate SS + Main Effects SS + Interaction SS + Residual Error

It is a particularly useful tool for putting the relative contributions of the numerical and category variables in global perspective. ANCOVA falls in a broader domain of General Linear Modeling (GLM), and Scheffé's procedure [9] of using Log(RMS) is applied here to mitigate the dependent variable being a measure of treatment *variance* rather than treatment mean.[8]

RESULTS

Accelerometer Mounting Methods

The accelerometer configuration mentioned above was not arrived at in a single step. The initial approach was to attach the triaxial accelerometer using the same hexagonal bracket that was developed for the Cobra, but drilled and tapped for the OH-58's threading. As with the Cobra, the bracket was installed directly above the stud's retaining nut. Unfortunately, after collecting initial flight data it became evident that some manner of temporal instability caused the accelerometer recordings to drift over several days of operation. This mounting method was rejected for this application, therefore, and the uniaxial bracket adapted for both types of accelerometer.[9] An advantage to the new method immediately became apparent in that the z-axis naturally positions radial to the annulus, the y-axis can be easily rotated to be tangential to the annulus, and the x-axis then aligns parallel to the rotor shaft.

The triaxial accelerometer was initially placed at a stud position immediately above the input pinion, and also closest to the engine. With both types of mounting bracket, large energies were produced in the tangential direction. This led to a series of static tap tests to determine the nature and source of the signal. It was determined that a mounting resonance existed that amplified a 5.1kHz frequency emanating from the shaft speed reduction gears in the engine. Hence, as might be expected, accelerometers mounted on the transmission inherit vibrations from other aircraft components. In an effort to minimize these effects, the triaxial was moved to a stud position further from the input pinion. There it was also observed that large signal energy occurred in the tangential direction, leading to the conclusion that the transmission has a torsional vibration at this engine frequency. Additional observations are discussed in the frequency analysis section below.

Table 3. Stationarity for OH-58 and AH-1

MANEUVER	PERCENT STATIONARY RECORDS	
	OH-58 Kiowa	AH-1 Cobra
A. Forward Flight, Low Speed	70.8%	55.6%
B. Forward Flight, High Speed	65.3%	61.1%
C. Sideward Flight Left	12.5%	22.2%
D. Sideward Flight Fight	9.7%	31.9%
E. Forward Climb, Low Power	50.0%	97.0%
F. Forward Descent, Low Power	16.7%	68.1%
H. Hover	30.2%	80.2%
I. Hover Turn Left	11.1%	59.7%
J. Hover Turn Right	15.3%	36.1%
K. Coordinated Turn Left	79.2%	80.6%
L. Coordinated Turn Right	83.3%	80.6%
M. Forward Climb, High Power	65.3%	86.1%
N. Forward Descent, High Power	22.2%	72.2%
Average Stationarity	40.6%	64.2%

Signal Stationarity

Stationarity refers to invariance of the statistical properties of a signal over time. To the extent that a vibration signal is known to be strongly nonstationary, caution needs to be exercised in performing certain basic operations, most notably synchronous signal averaging in either the time or frequency domains. The reason for this is that under nonstationary conditions averaging is very likely to smear non-linear effects in the underlying frequency distributions, with the result that the computed average does not converge on fixed population parameters. Differences between sample averages from a nonstationary process may be enigmatic, therefore, since apparent local changes related to nonstationarity may easily be confused with changes due to damage states, thereby triggering false alarms.

Table 3 provides an overall comparison of the OH-58 and AH-1 in terms of the observed stationarity of different in-flight maneuvers. The ground maneuver is excluded, although for each aircraft records taken on the ground with flat blade pitch were 100% stationary. Each of the 34-sec. recordings is broken into six successive "replications." In the case of the AH-1 Cobra, groups of 28 revolutions constituted a replication, whereas groups of 32 were used for the OH-58 Kiowa. These groups of shaft revolutions were

[8] Liberties have been taken with other assumptions that limit inferential conclusions. Results should be regarded as descriptive.
[9] Original prototypes for this bracket were obtained from the US Navy by GRC. The bracket design can not be retrofitted to the Cobra because of insufficient exposed threading.

examined with regard to the number of "runs" above and below their respective median RMS values, and a reference table used to determine if the observations would be expected from a binomial distribution with p=.5. A two-tailed test is used so that either too many or two few runs can potentially lead to the conclusion that a given replication is nonstationary.[10]

As seen in Table 3, the Kiowa produced appreciably fewer stationary records than did Cobra. What may have been a disappointing level of stationarity for the AH-1 (64.2%) was further reduced to 40.6% in the OH-58. It is likely that this is due to the large gross weight difference between the two aircraft, with inertial forces favoring the stationarity of the larger vehicle. Moreover, the relative distribution of stationarity across the 13 in-flight maneuvers is also very different between the two aircraft, with no systematic pattern emerging. The forward climb conditions that produced the highest stationarity in the Cobra produced mediocre results in the Kiowa. The maneuvers having the highest stationarity for both aircraft are the left and right coordinated turns. Overall, these were about 80% effective, well above the average for each aircraft, but whether this generalizes to other helicopters would need to be determined.

Fig. 3 provides a different perspective for understanding the stationarity results. Here the runs that were used in the tests for each replication are shown as a histogram for each aircraft. The lightly shaded areas correspond with examples that fall in the nonstationary regions. It is evident in both instances that nonstationarity is almost always produced by too few runs rather than too many. In other words, the RMS values tend to cluster below or above their respective medians longer than might be expected by chance. This is consistent with trends or low frequency variations occurring during the recording period.

Comparison of Triaxial Variance Using Torque and Rotor Speed as Covariates

Table 4 is a consolidation of six ANCOVAs for the PCA scores from each aircraft.[11] Each analysis was done in the same hierarchical manner described by Huff, Barszcz, et al, except that in this case only engine torque and rotor RPM were used as covariates, and interaction terms are extended to the third order. Higher order interactions are pooled with the error term. In essence, each ANCOVA is procedurally identical to first removing torque and RPM by linear regression, and then partitioning the residual variance using a five-factor, fixed-effects, analysis of variance (ANOVA) [8]. The Sum of Squares (SS) column is retained in the table from the original analyses, and the Percent Total SS columns are added to visualize the overall relative contribution of covariates, main effects, and interactions. A Percent "Corrected" SS column shows the distribution of variability after the linear covariate SS (i.e., Torque and RMS) is subtracted from the Total SS.

In contrasting the aircraft, two general observations may be made. First, the Grand Total SS across the three principal components is 3.6 times larger for the Cobra than the Kiowa. This is consistent with gross weight and power differences between the aircraft. Second, PC-1 accounts for a much larger percentage of the Grand Total SS on the Cobra (93.5%) than the Kiowa (75.3 %). Curiously, the absolute SS is just about the same when Torque and RPM are accounted for by linear regression. As was reported originally for the Cobra, moreover, Kiowa PC-2 and PC-3 scores generally show a larger Percent Total SS for main and interaction effects, respectively.

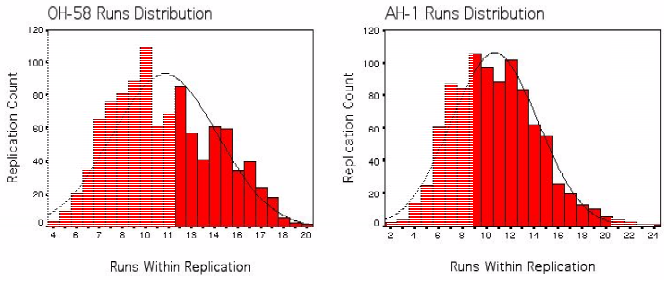

Figure 3. Distribution of Runs

Looking at Percent Corrected Total SS, although main effects account for the largest treatment variability, a consistently larger percentage is associated with 2- and 3-way *interactions* in the OH-58 than the AH-1. This is particularly evident on PC-3, and indicates that treatment effects are not as separable on the lighter aircraft. Finally, considering residuals for each PC it is apparent that except for PC-2 the ANOVA model has about the same modeling efficiency for the two aircraft after covariate influences are removed.

Because of the interaction effects on the OH-58, Table 5 is included to show the relative degree of variability accounted for by each treatment combination. In general, there is a remarkable similarity in the pattern of effects between the two aircraft, allowing for overall differences mentioned above. It is puzzling that for

[10] Cobra data were reanalyzed by combining runs across all six vibration channels. Percentages, therefore, differ somewhat from what was reported earlier.

[11] The triaxial on the Cobra was the same one reported in the earlier study, but results differ slightly. PCA scores were recomputed over the eight flights combined to make them comparable with the Kiowa's.

Table 4: Combined Sources of Variance for AH-1 and OH-58

Combined Sources	OH-58 Kiowa			AH-1 Cobra		
	Sum of Squares (SS)	Percent Total SS	Percent Corrected Total SS	Sum of Squares (SS)	Percent Total SS	Percent Corrected Total SS
PC-1						
Covariates	83.355	61.66		555.872	90.94	
Main Effects	24.461	18.10	47.20	29.261	4.79	52.85
2-Way Interactions	10.212	7.55	19.71	9.787	1.60	17.68
3-Way Interactions	10.845	8.02	20.93	9.356	1.53	16.90
Model	128.873	95.34		604.276	98.86	
Residual Error	6.303	4.66	12.16	6.965	1.14	12.58
Total	135.176	100.00	100.00	611.241	100.00	100.00
PC-2						
Covariates	0.185	0.47		0.198	0.49	
Main Effects	31.873	80.72	81.10	37.398	92.03	92.48
2-Way Interactions	2.838	7.19	7.22	1.174	2.89	2.90
3-Way Interactions	2.550	6.46	6.49	1.095	2.69	2.71
Model	37.446	94.83		39.866	98.10	
Residual Error	2.041	5.17	5.19	0.773	1.90	1.91
Total	39.487	100.00	100.00	40.638	100.00	100.00
PC-3						
Covariates	0.291	6.16		0.285	16.12	
Main Effects	0.855	18.11	19.30	0.738	41.74	49.76
2-Way Interactions	1.530	32.41	34.54	0.340	19.23	22.93
3-Way Interactions	1.481	31.37	33.43	0.224	12.67	15.10
Model	4.158	88.07		1.587	89.76	
Residual Error	0.563	11.93	12.71	0.181	10.24	12.20
Total	4.721	100.00	99.98	1.768	100.00	100.00
Grand Total	179.384			653.647		

both aircraft rotor RPM systematically accounts for a greater percentage of the Total SS than does torque on PC-2 and PC-3. It is as if PCA separates the influence of these two variables that are generally negatively correlated.[12] Of the main effects, Maneuver (M) is undoubtedly the dominant factor for each principal component.

Close examination of Table 5 reveals that of the 150 treatment combinations, 70 are significant even though only 1.5 would be expected to be so on the basis of chance ($\alpha = .01$).[13] Of these, only three (4.5%) are associated with the 66 combinations involving Replications (R), and 67 (79.8%) are associated with the remaining 84 combinations. This implies that nonstationary trends mentioned earlier are largely contained within the approximate 5.7 sec. recording periods for each replication.

Comparison of Four Uniaxial Accelerometers on the OH-58 Kiowa

A primary motivation for installing multiple uniaxial accelerometers near the annulus gear is to support planetary signal decomposition. The general idea is that multiple recordings may be used to decompose the signal into individual planet signatures more readily than just one, and also that it may be useful to incorporate several sections of the annulus gear in the data for damage identification. In preparation for OH-58 flight research to be done next year on this subject, certain analyses are summarized here. Two issues of particular interest are: (i) whether the signals from sensors at different locations behave in the same way, and (ii) the extent to which *nonstationarity* influences the results. The latter issue is important because long temporal records needed for planetary analysis are particularly subject to the vagaries of nonstationarity.

Table 6 summarizes the results of analyses performed separately on stationary vs. nonstationary cases for each of the four radial accelerometer channels (A1, A2, A3, A6). Here, the ANCOVA is used to model only covariate and main treatment effects; all interactions are pooled with residual error. To do these analyses, the records were first partitioned in accordance with the histogram in Fig. 2b, where the nonstationary records are shown in the shaded area.

For reasons that are not apparent, the four accelerometers produce different absolute levels of RMS variability as shown by the SS entries. It is also quite apparent that nonstationary records produce a greater SS across all accelerometers, and that the

[12] Engine torque and shaft speed correlate negatively because of speed regulation of the aircraft engine.
[13] Statistical significance should be regarded with caution in view of liberties taken with parametric modeling assumptions.

Table 5: Percentage of Total Sum of Squares for Each Principal Component

	PC-1		PC-2		PC-3	
Source of Variance	**AH-1**	**OH-58**	**AH-1**	**OH-58**	**AH-1**	**OH-58**
	Percent Total SS	**Percent Total SS**	**Percent Total SS**	**Percent Total SS**	**Percent Total SS**	**Percent Total SS**
(Covariates)						
TORQUE	90.80 *	59.56 *	0.02	0.00	0.16 *	0.34 *
RPM	0.14 *	2.10 *	0.46 *	0.47 *	15.95 *	5.83 *
(Main Effects)						
MANEUVER (M)	4.55 *	16.71 *	91.38 *	80.01 *	14.76 *	16.39 *
ORDER (O)	0.08 *	0.11 *	0.03	0.09	0.70 *	0.04
PILOT (P)	0.00	0.01	0.13 *	0.23 *	0.19 *	1.29 *
REPLICATE (R)	0.01	0.01	0.01	0.05	0.12	0.23
SET (S)	0.15 *	1.25 *	0.48 *	0.34 *	25.96 *	0.15
(2-Way Interactions)						
M * O	0.84 *	1.31 *	1.17 *	1.85 *	2.66 *	5.06 *
M * P	0.27 *	3.26 *	0.31 *	2.31 *	5.94 *	8.83 *
M * R	0.15	0.41	0.27	0.76	2.32 *	1.25
M * S	0.20 *	2.15 *	0.80 *	1.33 *	5.94 *	15.25 *
O * P	0.03 *	0.31 *	0.03	0.05	0.01	0.08
O * R	0.02	0.03	0.03	0.03	0.25	0.16
O * S	0.02	0.07	0.00	0.13 *	0.35 *	0.39 *
P * R	0.01	0.03	0.03	0.01	0.18	0.25
P * S	0.03 *	0.22 *	0.18 *	0.62 *	0.55 *	1.60 *
R * S	0.01	0.02	0.06	0.04	0.24	0.09
(3-Way Interactions)						
M * O * P	0.40 *	1.66 *	0.41 *	1.18 *	0.81	4.26 *
M * O * R	0.23	0.97	0.37	1.02	1.79	2.22
M * O * S	0.49 *	1.02 *	0.78 *	0.91 *	3.08 *	3.18 *
M * P * R	0.13	0.52	0.35	0.79	1.58	1.27
M * P * S	0.16 *	2.70 *	0.20 *	1.27 *	1.05 *	17.84 *
M * R * S	0.09	0.47	0.43 *	0.64	3.15 *	1.32
O * P * R	0.03	0.12	0.04	0.06	0.36	0.24
O * P * S	0.00	0.09	0.03	0.24 *	0.31 *	0.35 *
O * R * S	0.01	0.11	0.04	0.07	0.12	0.24
P* R * S	0.00	0.10	0.03	0.05	0.20	0.17
Model	98.86 *	95.34 *	98.10 *	94.83 *	89.76 *	88.07 *
Residual Error	**1.14**	**4.66**	**1.90**	**5.17**	**10.24**	**11.93**
Total *	100.00	100.00	100.00	100.00	100.00	100.00

* (α=.01)

residual error of the general linear model is larger in each case. In other words, stationarity has a clear advantage in being associated with lower signal variability and greater model predictability. Finally, there is no reason to believe that A6, i.e., the z-axis of the triaxial, produced different output than the uniaxial equivalents; indeed, it behaved similar to A2.

Frequency Analyses of Aircraft and Test Platform

Three panels in Fig. 4 show a representative amplitude spectrum for each of the three platforms. The spectra from the OH-58 Cobra and AH-1 Cobra flight experiments are computed using a single forward climb, low power maneuver that is averaged over the 34-sec. recording interval. The averaged spectrum for the OH-58 test rig is taken from a 34-sec. medium torque, low mast lift, and low mast bending force condition. A decibel (i.e., Log) scale is used to enhance low amplitude frequencies, also making leakage byproducts evident [14].

Labels on the spectral plots clearly demonstrate the presence of expected transmission frequencies for the bevel gears and the planetary gears, as well as higher-order harmonics below the 18kHz cutoff of the anti-aliasing filter.[14] What may be meaningful sidebands and other high amplitude frequencies have yet to be identified. With regard to the OH-58c, the main 5.1kHz turbine engine gear mesh frequency and its harmonics are evident for the flight data (Fig. 4a). These do not appear in the spectral plot for the test rig data (Fig. 4c), but in other respects the two plots are similar. With regard to the AH-1, (Fig 4b) a distinction is drawn between frequencies generated by the upper and lower planetary stages.

Using the components of variance (i.e., power) grouping method discussed earlier, Table 7 contrasts the parsing of signal variance of the four averaged radial channels on the aircraft with the single sensor output on the test rig that uses the same mounting bracket. With the exception of the engine frequencies, which account for a sizeable percentage of Total Mean Square (MS) on the aircraft (21.68%), the planetary and bevel-gear percentages appear very similar to the test rig. Ironically, even though the aircraft had additional engine sources to increase signal power, the test rig had a larger Total MS. This may be due to low frequency components derived from the test rig's unique feedback apparatus—a hypothesis currently being explored. It is also notable, on both the OH-58c aircraft and the test rig, that the pinion gears represented about the same proportion of the Total MS as the planetary gears (≈16%).

Table 8 shows comparable information for the AH-1, which is averaged over the three channels of the triaxial accelerometer reported in previous analyses. As can be seen, the Total MS is two orders of magnitude larger than the OH-58's. Even though the accelerometer is mounted close to the upper planetary stage, twice the percentage of signal energy is derived from the lower stage. Unlike the OH-58c, only .52% of the Total MS is associated with the pinion mesh frequencies, which may be due to physical distance or other structural transfer effects. Finally, there is a much larger proportion of residual (i.e., unexplained) variance (83%) for the AH-1 than for the OH-58 (45%) based on known mesh frequencies. This suggests that additional sources of variability may be present, which could be associated with other driven gears, engine components, tail rotor components, etc.

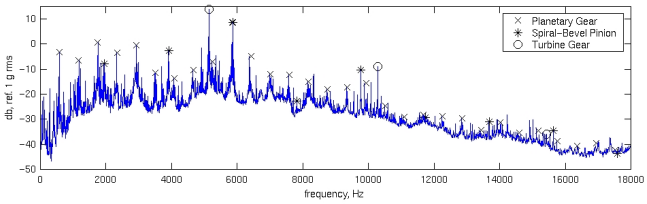

Figure 4a. Averaged Spectra from OH58c (uniaxial).

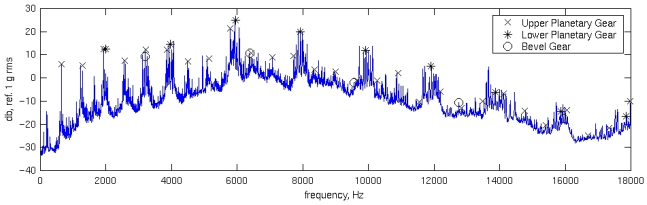

Figure 4b. Averaged Spectra from AH-1 (triaxial).

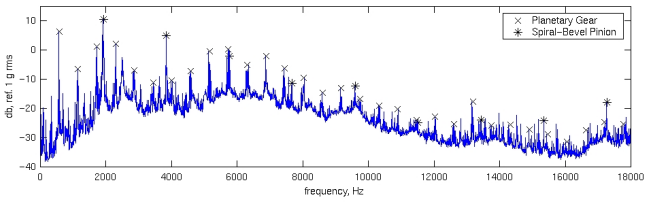

Figure 4c. Averaged Spectra from GRC Test Facility (uniaxial).

[14] Although not visible in the chart, the planetary mesh frequency is actual spread over several frequency bands as expected.

Table 6: Radial Channel Analyses on OH-58 for Stationary and Nonstationary Records

		OH-58c Kiowa Radial Channels					
		Stationary			Nonstationary		
		Sum of Squares (SS)	Percent Total SS	df	Sum of Squares (SS)	Percent Total SS	df
Log(A1)	Covariates	6.279	37.99%	2	4.415	14.77%	2
	Main Effects	7.318	44.28%	21	18.766	62.79%	21
	Model	13.597	82.28%	23	23.18	77.56%	23
	Residual Error	2.93	17.73%	361	6.705	22.44%	527
	Total	16.526	100.00%	384	29.886	100.00%	550
Log(A2)	Covariates	14.492	60.07%	2	13.52	52.21%	2
	Main Effects	6.477	26.85%	21	7.402	28.58%	21
	Model	20.97	86.92%	23	20.922	80.80%	23
	Residual Error	3.156	13.08%	361	4.973	19.20%	527
	Total	24.126	100.00%	384	25.895	100.00%	550
Log(A3)	Covariates	3.432	29.75%	2	1.027	8.10%	2
	Main Effects	6.175	53.52%	21	7.022	55.40%	21
	Model	9.607	83.26%	23	8.049	63.50%	23
	Residual Error	1.931	16.74%	361	4.626	36.50%	527
	Total	11.538	100.00%	384	12.675	100.00%	550
Log(A6)	Covariates	7.918	58.03%	2	10.336	51.92%	2
	Main Effects	3.074	22.53%	21	4.11	20.64%	21
	Model	10.992	80.56%	23	14.447	72.57%	23
	Residual Error	2.654	19.45%	361	5.462	27.43%	527
	Total	13.645	100.00%	384	19.909	100.00%	550

Table 7: OH-58c and Test Rig Spectral Variance Components

	OH-58c Aircraft Average 4 Radial Channels			OH-58c Test Rig Sensor #3 Radial		
Source	Variance (MS)	df	Percent Total MS	Variance (MS)	df	Percent Total MS
Planetary	17.98	70	17.48	23.38	70	13.79
Pinion - Gear	15.86	18	15.42	30.14	18	17.77
Engine	22.29	6	21.68			
Residual Variance	46.70	8098	45.42	116.07	8104	68.44
Total Mean Square (MS)	102.83	8192	100.00	169.59	8192	100.00

Table 8: Cobra Spectral Variance Components

	AH-1 Cobra Aircraft Average 3 Triaxial Channels		
Source	Variance (MS)	df	Percent Total MS
Upper Planetary	691.89	60	5.59
Lower Planetary	1376.99	12	11.12
Pinion - Gear	64.72	10	0.52
Residual Variance	10247.73	8110	82.77
Total Mean Square (MS)	12381.33	8192	100.00

CONCLUSIONS AND FUTURE RESEARCH

In the present study an effort was made to measure transmission vibrations from an OH-58c Kiowa helicopter and to compare them with results previously obtained from an AH-1 Cobra and an OH-58c test rig. In the process, issues were addressed that include instrumentation, methodology and analysis. Although gratifying progress was made at each level, it is most important to highlight what has been learned for future HUMS development.

The combined weight of Cobra and OH-58 data do not support conventional wisdom that flight conditions in general, or maneuvering states in particular, produce sufficiently stationary signals for reliable early detection of damage patterns. On the contrary, there is every indication that traditional time-synchronous averages will contain enough variability due to non-stationarity to compromise the early identification of damage, and very possibly induce high false alarm rates. Although only two aircraft have been studied to date, it is speculated that there is a strong relationship between aircraft gross weight and the character of the vibration signals that are available for HUMS processing. Depending on sensor location, for example, the Cobra easily produced signals that exceed current industry standards for HUMS accelerometers (±500g). This may be exacerbated on larger aircraft, where the potential for clipping will require very careful signal gain management.

Analytical precepts that have been explored in this and earlier studies support the unifying theme of partitioning signal variance based on the engineering and operational knowledge of the system. This is coupled with the view that damage identification algorithms are essentially methods for detecting changes in the variance properties of the signal, and that partitioning will greatly improve the success of subsequent signal detection in terms of maximizing "hits" and minimizing "false alarms."

The current findings underscore the possibility of removing large amounts of signal variance that can be predicted *a priori*, from engineering or operational knowledge. As shown in the present cases, a very large proportion of variance can be partialed out of the signals simply based on knowledge of gear mesh frequencies, engine torque, and rotor RPM. Other engineering knowledge, not currently available to the authors, as well as flight dynamic factors, may further lower the residual variance to levels where trustworthy damage detection is feasible.

Based on these observations, ongoing research at NASA Ames and NASA Glenn is now being directed to signal processing under free-flight conditions. To circumvent the possible limitations of conventional signal averaging, a modified method called Discontinuous Time Synchronous Averaging (DTSA) is being explored. This technique averages data in the time or frequency domains from shaft revolutions that satisfy pre-defined criteria, e.g., RPM, torque, aircraft attitudes, etc.[15] The existing flight research database is being used to explore the potential benefits of the method. Free-flight studies will be conducted, however, to answer basic questions about data acquired during transient maneuvering states, and to obtain false alarm statistics for various detection algorithms. An improved system called HealthWatch-II is under development that will perform DTSA in continuous flight, as well as apply a battery of candidate metrics for false-alarm evaluation.

As final comments, vehicle health monitoring equipment, e.g., accelerometers, cables, brackets, and so forth, are often perceived as easily retrofit to a vehicle. In the case of high frequency vibration monitoring this is hardly the case. The identification of sensor mounting locations is at best a matter of circumstance that in no way assures optimal placement or effectiveness. There would seem to be every reason, therefore, for engine, transmission and other component manufacturers to make provision for sensor attachment at the design stage, or to modify current designs with optimal sensor placements in mind. In this way, it should be possible to control resonant frequencies, minimize the need for special mounting brackets, and take advantage of the benefits of multi-channel accelerometers. A related matter is the need for making vehicle state information, now only available to certain avionics or cockpit displays, also accessible for on-board diagnostic and reasoning systems. Again, this issue is best handled at the design stage.

Acknowledgement

The authors would like to thank Dr. Eugene Tu, Manager of NASA's Information Technology Base program, for providing support for conversion of HealthWatch to the OH-58. We would also like to complement the Army Flight Projects Office (FPO) for the coordination of all aircraft instrumentation and flight support activities. Special thanks is given to Dr. Upender Kaul for statistical data preparation, and to Larry Cochrane, California Signal Processing Associates (Sigpro), for outstanding HealthWatch technical support.

[15] A US Patent application has been filed for DTSA.

REFERENCES

1. Huff, E.M., Barszcz, E. *et al. Experimental analysis of steady-state maneuvering effects on transmission vibration patterns recorded in an AH-1 Cobra helicopter* in *American Helicopter Society Annual Forum*, 2000, Virginia Beach, VA.
2. Hess, A., B. Hardman, and C. Neubert. *SH-60 helicopter integrated diagnostic system (HIDS) program experience and results of seeded fault testing* in *American Helicopter Society 54th Annual Forum*, 1998, Washington, D.C.
3. Kershner, S.D., J.B. Johnson, and M.D. Gamauf. *Sikorsky support to commercial health and usage monitoring systems: a summary of four months of support* in *American Helicopter Society 53rd Annual Forum*, 1997, Virginia Beach, VA.
4. Larder, B.D. *An analysis of HUMS vibration diagnostic capabilities* in *American Helicopter Society 53rd Annual Forum*, 1997, Virginia Beach, CA.
5. Huff, E.M., Tumer, I.Y. *et al. Experimental analysis of mast lifting and mast bending fores on vibration patterns before and after pinion reinstallation in an OH58 transmission test rig* in *American Helicopter Society's 56th Annual Forum*, 2000, Virginia Beach, VA.
6. Masters, T., *Neural, Novel & Hybrid Algorithms for Time Series Prediction*. 1995, New York: Wiley.
7. Johnson, R. and D. Wichern, *Applied multivariate analysis*. 1992, New York, NY: Prentice Hall.
8. Montgomery, D.C., *Design and analysis of experiments*. 1991: John Wiley & Sons.
9. Sheffe, H., *The Analysis of Variance*. 1st Edition ed. 1959, New York: Wiley.
10. Tumer, I.Y. and E.M. Huff. *Using triaxial accelerometer data for vibration monitoring of helicopter gearboxes* in *ASME Design Engineering Technical Conferences, Mechanical Vibration and Noise Conference*, 2001, Pittsburgh, PA.
11. Bendat, J. and A. Piersol, *Random Data: Analysis and measurement procedures*. 1986, New York, NY: John Wiley &Sons.
12. Lewicki, D.G. and J.J. Coy, *Vibration characteristics of OH58a Helicopter main rotor transmission*, 1987, NASA Glenn Research Center: Cleveland, Ohio.
13. Smith, J.D., *Gear Noise and Vibration*. 1999, New York, NY: Marcel Dekker.
14. Oppenheim, A.V. and A.S. Willsky, *Signals and Systems*. 1997: Prentice Hall.